

LABORATORY MEASUREMENTS OF COMETARY  
PHOTOCHEMICAL PHENOMENA

William M. Jackson  
Howard University  
Washington, DC 20059

Abstract

Laboratory experiments are described that provide fundamental information about photochemical processes in comets. The yield of cometary radicals such as CN, OH, etc. can be determined as a function of photolyzing wavelength. Quantum state distributions of the internal energy of the cometary radicals can also be measured as a function of wavelength permitting one to define the recoil velocity of the fragments. This type of information supplies the data needed for more elaborate models to interpret the data being obtained on comets.

Introduction

The photodissociation of parent molecules in the coma of comets takes place under conditions that are considerably different than those of most laboratory studies. The pressures in the coma of comets varies from  $10^{-3}$  torr to essentially zero while most laboratory studies on photodissociation are done at substantially higher pressures. Furthermore, in the laboratory one usually uses light at a single well defined wavelength or band to photodissociate the parent compound, whereas in comets many different wavelengths from the sun are simultaneously impacting the molecules in the coma. Yet despite these problems, it is essential for cometary astrophysicists to have a complete knowledge of the photodissociation processes so that they can infer the identity of the parent processes responsible for the various daughter radicals.

The detailed knowledge of the dynamics of photodissociation processes that occur in  $H_2O$  photolysis has given the cometary astrophysicist reasonable confidence that water is responsible for most of the OH and H observed in comets. Further inference of the parent molecules that are responsible for the observed daughters in comets will require even more detailed laboratory information. We have built a laboratory instrument that allows the experimenter to measure the dynamics of the photodissociation processes as a function of the wavelength of the photolysis light source. This instrument can thus yield the kind of information that will permit us to do detailed analysis of new observational data obtained from comets. With this experimental information better theoretical models of the coma may be constructed (with a minimum of assumptions) to explain these observations.

Experimental

A schematic diagram of the apparatus that has been built to study the details of photochemical dynamics is given in Figure 1. It consists of a vacuum ultraviolet monochromator with a single slit and holographic grating. The entrance slit of the monochromator is the image of a VUV flashlamp. With these design innovations one can obtain  $10^{11}$  photons/flash in a  $10\text{\AA}$  bandpass with a FWHM pulse width of 100 nsec. This kind of performance requires only a modest input energy of 1.6 J/flash. The source is bright enough so that wavelength dependent photodissociation processes can be observed.

The sensitive detection scheme that has been used in these studies employs a tunable dye laser to excite daughter molecules in a given rotational level. The dye laser acts the same way the sun does in comets, it lights up the daughter radicals. The fluorescence from the radicals is recorded as a function of wavelength yielding an excitation spectra that provides both qualitative and quantitative identification of this species. The quantitative sensitivity is such that densities as low as  $10^5/\text{cm}^3$  in a given rotational level can be observed. If the daughter radicals are spread over 30 or 40 rotational levels, a good signal to noise ratio can be obtained with total radical densities as low as  $10^8$  to  $10^9/\text{cm}^3$ .

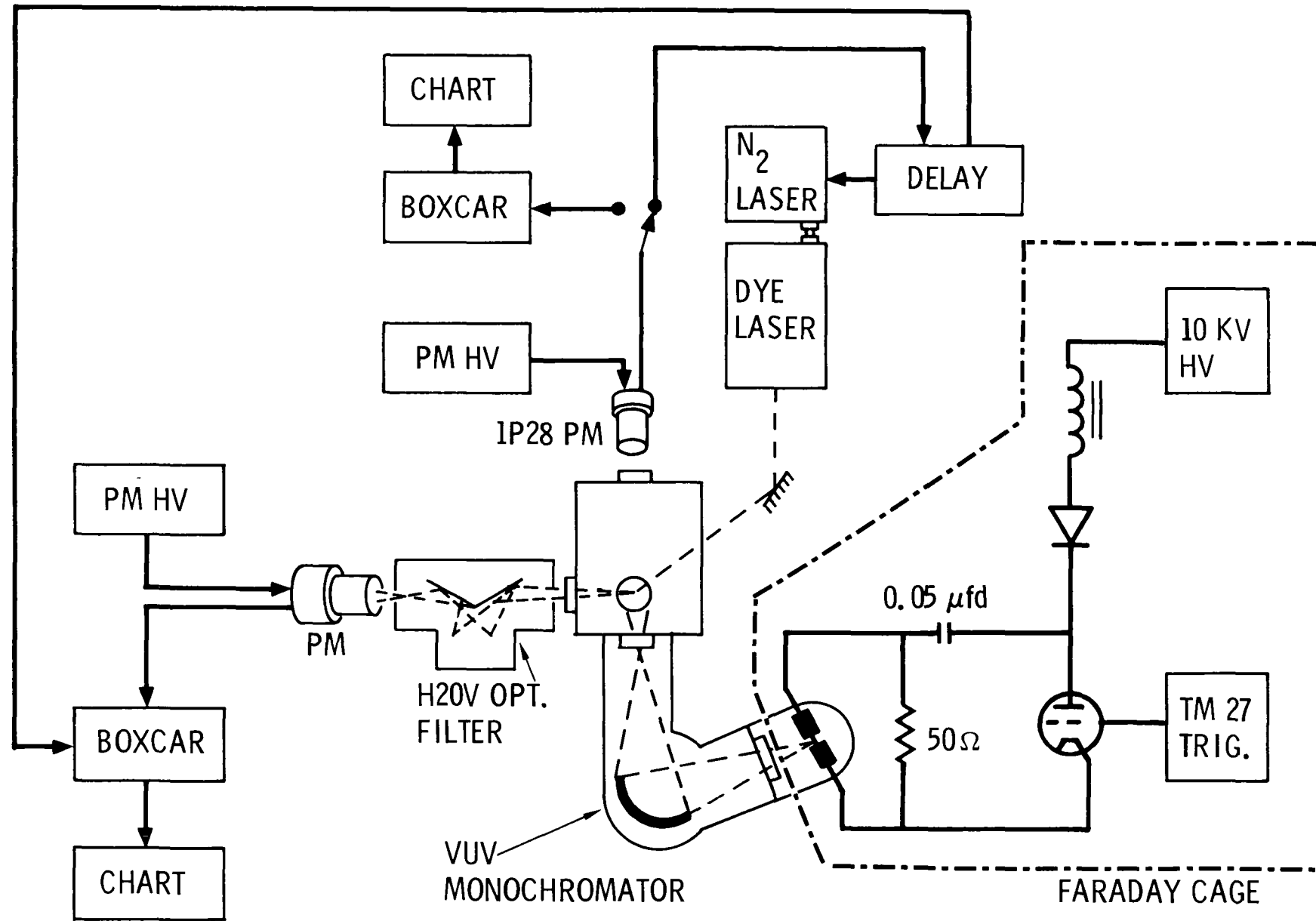


Figure 1. Photofragment Monochromator.

While we cannot duplicate the conditions that occur in the coma of comets with this apparatus, we can obtain information in a way that precludes the necessity of doing this. Since we are using a pulsed flashlamp we can arrange to detect fragments in times that are short compared to the average collision time for a daughter radical. For example at 1 torr, or  $3 \times 10^{15}$  molecules per  $\text{cm}^3$ , the time between collisions is of the order of 100 nsec. By reducing the pressure to a 0.10 torr, this increases to  $1 \mu$  sec. If we detect the radical within the 100 nsec only 10 percent of the molecules will have undergone any collisions, and the observed quantum state distribution should reflect the original quantum state distribution of most of the daughter radicals.

## Results

### a. Photodissociation of $\text{C}_2\text{N}_2$ :

The first molecule that was intensively studied with this apparatus was cyanogen. It is an ideal first candidate since it produces large amounts of CN radicals in the ground  $\chi^2\Sigma^+$  state when photolyzed between 160nm and 154nm (1). This is also the spectral region where 71 percent of these molecules will be dissociated by solar radiation (2). The molecule is thought to be linear in the excited state (3) and it is suspected that the bands shown in Figure 2 at 160, 158, and 154 nm are due to vibrational progressions in the excited state. The splitting inside the bands have been ascribed to a Renner-Teller interaction (3). The observed spectrum results from the electronic excitation of ground state cyanogen to the  $\text{C}^1\Pi_u$  state (3), while the vibrational progression corresponds to successive excitations of the symmetric CN stretching frequency. All of the levels of the  $\text{C}^1\Pi_u$  that are accessed by photolysis in this work are 4397 to 9881  $\text{cm}^{-1}$  above the dissociation limit that leads to two CN radicals, one in the  $\text{A}^2\Pi$  state and the other in the  $\chi^2\Sigma$  state.

Typical spectra that have been determined with the latest version of the photofragment monochromator are shown in Figure 3. The spectra were taken with a 100 nsec delay between the peak of the flash lamp output and the peak of the output from the dye laser. The signal to noise ratio in this spectra is comparable to the signal to noise ratio obtained previously (4) with a broad band flash lamp. It is considerably better than that originally obtained with the photofragment monochromator. The data may be conveniently analyzed by plotting the population of individual rotational levels as a function of the rotational energy. An example of such a plot is given in Figure 4.

This data shows some curvature at energies corresponding to the lower rotational levels. Similar behavior has been observed with the broad band flash lamp and, as will be shown later, with other systems involving the CN radicals.

The observed points in Figure 4 may be fitted with the curve corresponding to the sum of two Boltzman exponential functions. From the curve, two "temperatures" may be derived which are useful for later data analysis. The lower temperature could be a reflection of the increased probability of collisional relaxation to the lower energy levels. It has been suggested (5) that the probability of rotational relaxation decreases as the energy difference between the levels increases. The present data would support this suggestion since in all cases where curvature is observed, it is the lower rotational levels that are cooler than the upper levels. Ashford and Simons (6) however have shown that two temperatures result when collisional relaxation occurs during photolysis. In their system, the time observation is determined by the lifetime of the  $\text{B}^2\Sigma$  state which is 65 nsec (7). In our system the lifetime of the observation is determined by the delay between the flash lamp and the laser which is typically 0.1 sec. The total pressure is also important in determining whether rotational relaxation occurs. A good measure of this probability is the product of the characteristic observation time and the total pressure. In the present system this product is of the order of  $1.5 \times 10^{-2}$  torr-sec. Ashford and Simons have demonstrated that at "characteristic observation times" such as this no quenching occurs. It is unlikely that rotational relaxation is responsible for the deviation observed at low rotational energies so that this curvature probably reflects the fundamental photodynamics of the process.

The other product of the photolysis of  $\text{C}_2\text{N}_2$  is a CN radical in the  $\text{A}^2\Pi$  state. No previous measurements have been able to determine the rotational distribution of this state. The first laser excitation spectra of the Le Blanc ( $\text{A}^2\Pi \rightarrow \text{B}^2\Sigma$ ) system is displayed in Figure 5. This is also the first laser fluorescence spectra obtained for the lowest vibrational level of this system. Spectra similar to this have been obtained at several photolysis wavelengths and



C<sub>2</sub>N<sub>2</sub> PHOTOLYSIS at 158.7 nm, 600 ns delay, and 150 mtorr

$x^2\Sigma \rightarrow B^2\Sigma$   
Transition

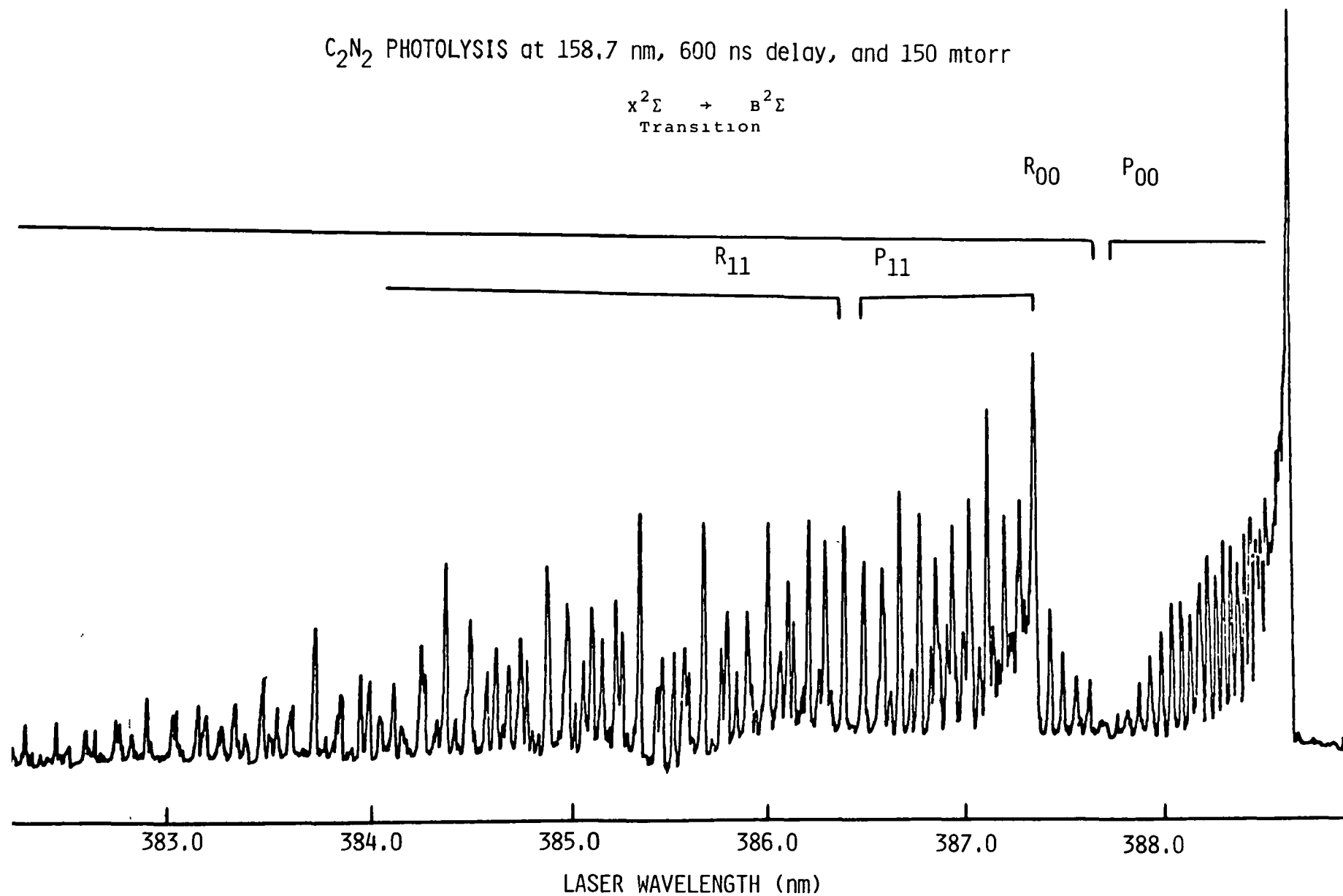


Figure 3. Laser Induced Fluorescence Spectra of the CN radical produced in the VUV photolysis of C<sub>2</sub>N<sub>2</sub> at 158.6 nm with a 20 nm FWHM bandwidth. The x axis is the dye laser wavelength and the y axis is the fluorescence intensity as viewed at right angles to both the laser light and the photolysis light.

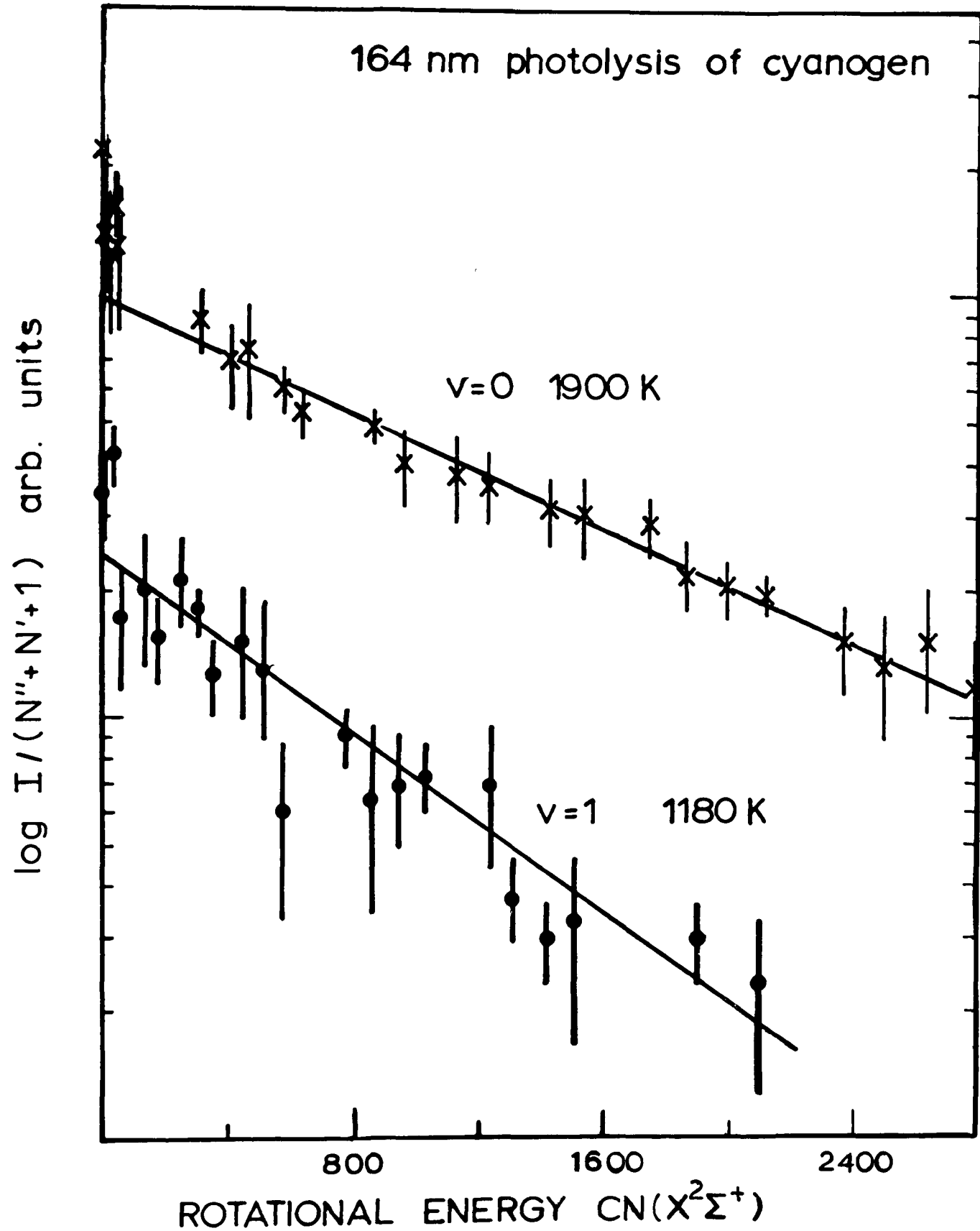


Figure 4. Boltzmann type plot of the rotational distribution of the CN radical produced in the photolysis of  $\text{C}_2\text{N}_2$ . The y axis is the log of the rotational population and the x axis the rotational energy of the levels.

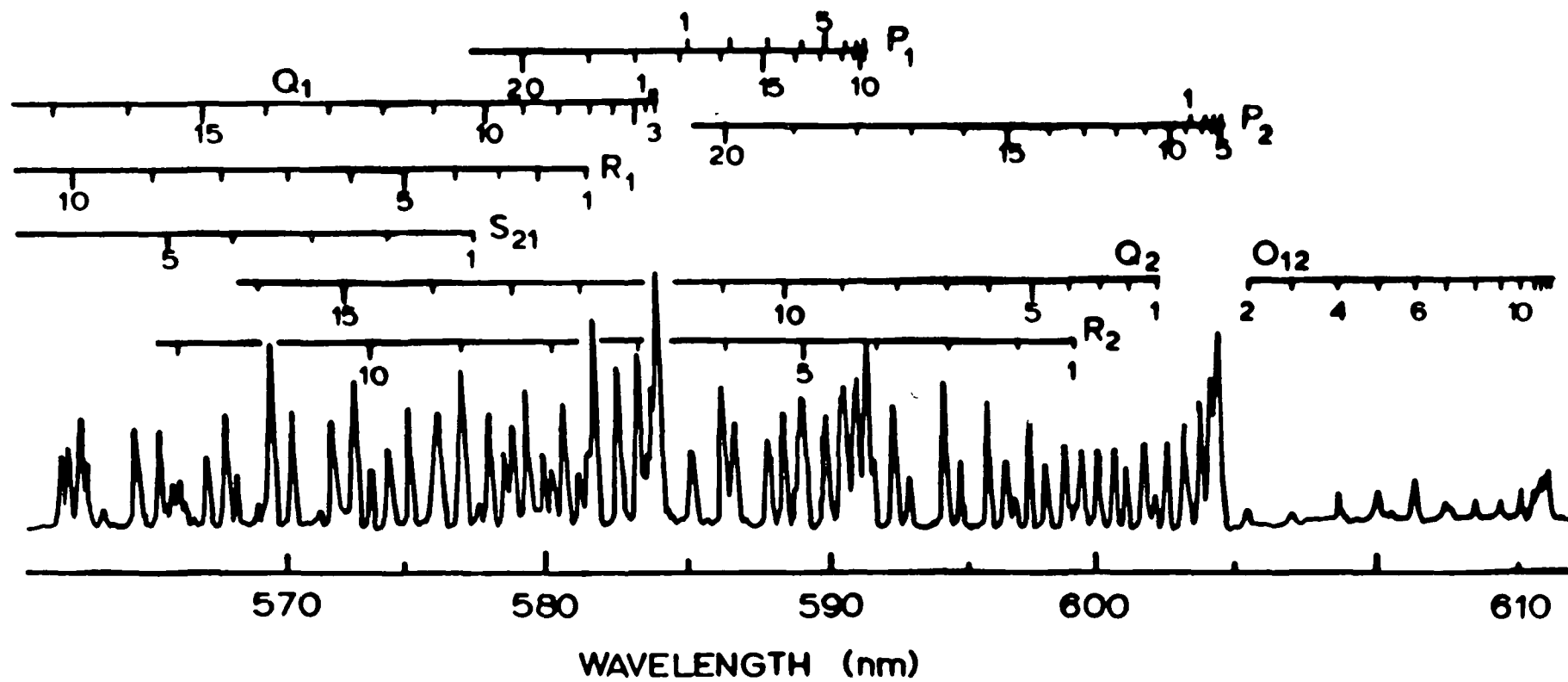


Figure 5. Laser induced fluorescence spectra of the LeBlanc system of CN. The transition that is being observed is from the  $v' = 0$  of the A state to the  $v' = 0$  of the B state of CN.

they have been analyzed to obtain the relative population of individual rotational levels. These populations can then be plotted in a Boltzmann plot to obtain the rotational temperature of the  $A^2\Pi$  state radicals.

The Boltzmann plot for the first data obtained at 159 nm is shown in Figure 6. The data is not yet good enough to determine whether this plot also shows curvature but it does indicate that the rotational temperature of the  $A^2\Pi$  state is greater than 1050°K. The  $X^2\Sigma$  state fragment however, had a rotational temperature of 1950°K which is almost a factor of two greater than the  $T_{rot}$  for the  $A^2\Pi$  state. If further analysis substantiates these observations, the data may suggest that the moment of inertia at the end of the molecule that becomes the  $A^2\Pi$  is larger than the end that becomes the  $X^2\Sigma$  state fragment. This is consistent with the idea that the vibrations that are excited in the  $C^1\Pi_u$  state of  $C_2N_2$  are the asymmetric stretch frequencies rather than the symmetric stretch frequencies. In the latter case the one would expect that the deformation would lead to the same internuclear distance between the C-N bond for both ends of the molecules. This interpretation is also in accord with the observation that the rotational temperature of the CN( $X^2\Sigma$ ) fragment is independent of the excitation energy in the  $C^1\Pi_u$  state of  $C_2N_2$ . If this suggestion is correct then the  $A^2\Pi$  state rotational temperature will increase with the excitation wavelength since the compression in this part of the molecule will have to increase.

Once the dynamics of photodissociation are understood, the photofragment spectrometer may also be used to obtain the relative quantum yield for radical production as a function of wavelength. This can be accomplished by setting the laser wavelength on the band head and scanning the photolyzing monochromator. Data obtained in this manner are shown in Figure 7. The different data points correspond to the relative yields determined using different band heads and rotational lines. All of the data agree, as it should, since it has been determined that the rotational temperature of this state does not change with wavelength. If the absolute quantum yield was known for one of the points in the diagram then the absolute quantum yield could be determined over the range of the scan. This is valuable information when one wants to do modeling calculations for cometary atmospheres since it allows one to correct for the effects of the broadband radiation from the sun. The profile of the band follows the profile of the absorption band which indicates that the true absolute quantum yield is probably one throughout this wavelength region.

#### b. $C_2HCN$

The quantum state distribution of the CN fragment produced from the broad band flash photolysis of cyanoacetylene was first reported by R. Cody and M. Sabety-Dzvonik (8). In that study they found that most of the CN radicals were formed in the  $v''=0$  level of the  $X^2\Sigma$  state. No  $A^2\Pi$  state was formed, and the rotational distribution could be assigned a "temperature" of approximately 1800°K. The spectra of cyanoacetylene (3) shown in Figure 8 indicate numerous absorptions in the wavelength region above 140 nm where Cody et al. performed their photolysis. The upper state of  $C_2HCN$  is thought to be linear. Vibrational progressions can be identified which are thought to correspond to the CN  $\nu_2'(\sigma^+)$  antisymmetric stretch frequency which should be strongly coupled to  $C\equiv C$  triple bond stretching frequency. This should support energy transfer to this part of the molecule and thus enhance energy randomization. Enhanced energy randomization would mean that more and more energy will go into the bending vibrations of the molecule as the photolysis energy is increased.

One of the states in this region near the long wavelength absorption band shows some evidence of Rydberg character. It was also of interest to determine if any evidence could be found in the dynamical results which would reflect the presence of these different electronic states.

A typical laser excitation spectra obtained by photolyzing 60 microns of  $HC_3N$  at time delays of 0.8  $\mu$ sec and at different wavelengths is shown in Figure 9 while the rotational population versus the rotational energy is shown in Figure 10. This latter spectra shows that within the accuracy of the data the rotational distribution is independent of the photolysis wavelength.

The remarkable thing about the observed rotational distributions for both  $C_2N_2$  and  $C_2HCN$  is that in both cases they appear to be independent of the photolyzing wavelength. Or put in another fashion the rotational distribution does not appear to depend upon the amount of energy that is available for distribution among the fragments.

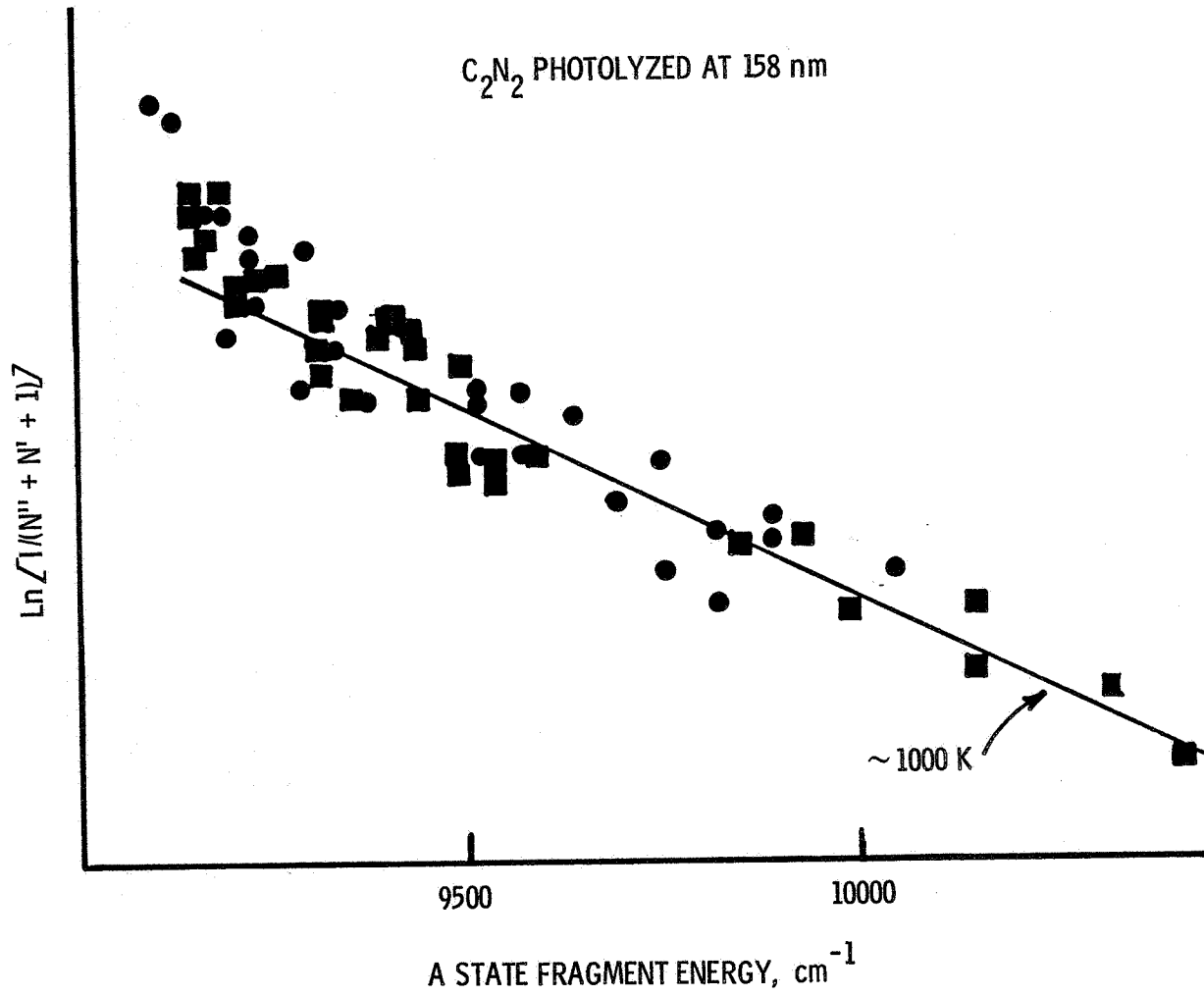


Figure 6. A Boltzmann type plot of the A state population of CN obtained from the LeBlanc system.

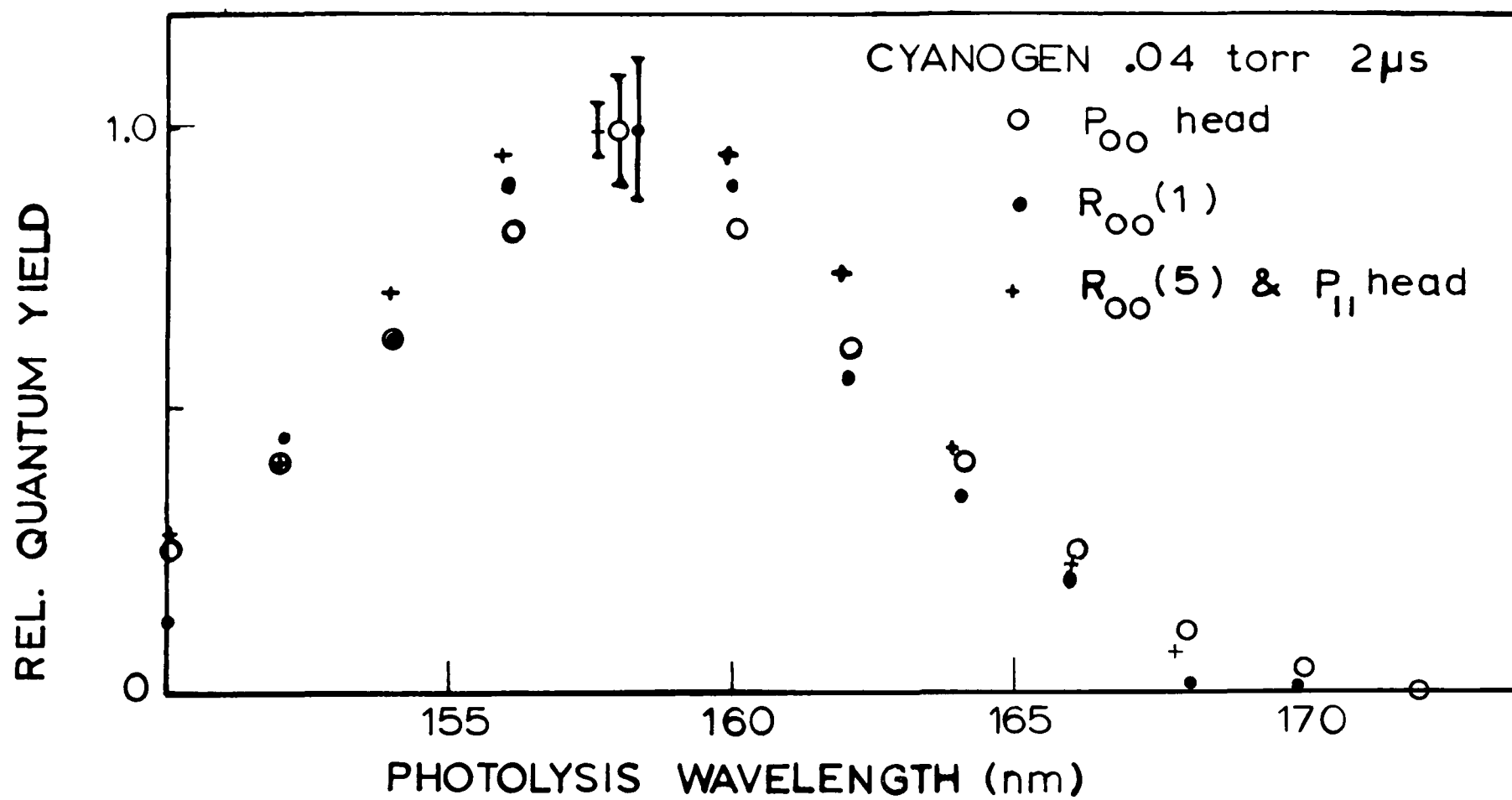
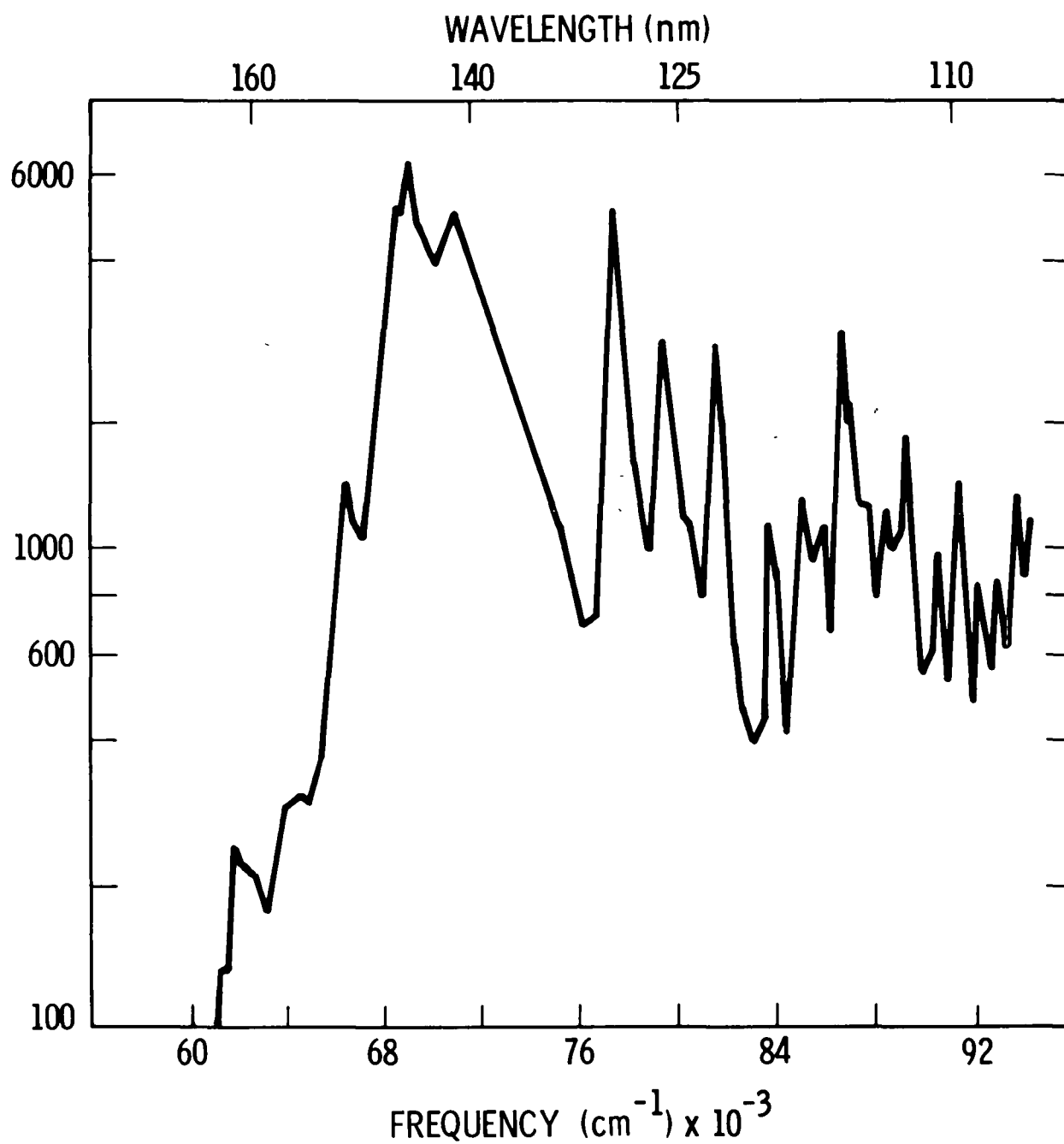


Figure 7. Quantum yield measurements of the X state of CN produced in the photolysis of C<sub>2</sub>N<sub>2</sub>.



ABSORPTION SPECTRUM OF CYANOACETYLENE  
(CONNERS ET AL JCP 60 (1974) 5011)

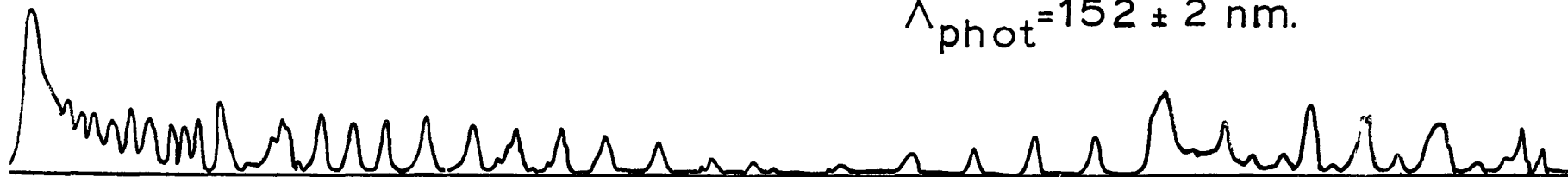
Figure 8. Dyanoacetylene absorption spectra.

CYANOACETYLENE  $CN(X^2\Sigma^+)$  PHOTOFRAGMENT SPECTRA

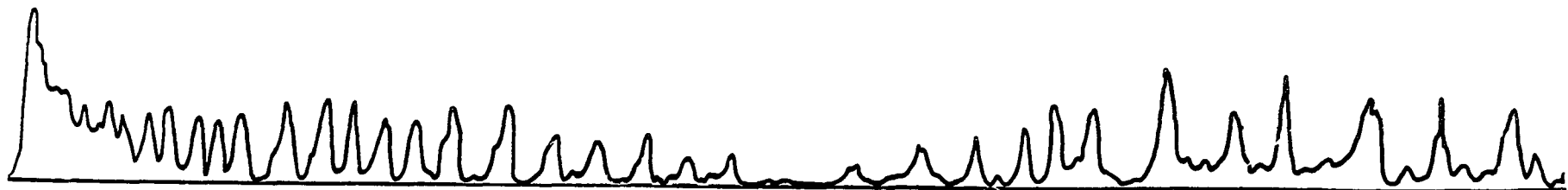
0.06 TORR

0.8  $\mu s$  DELAY

$\lambda_{phot} = 152 \pm 2$  nm.



160  $\pm$  2 nm



164  $\pm$  2 nm

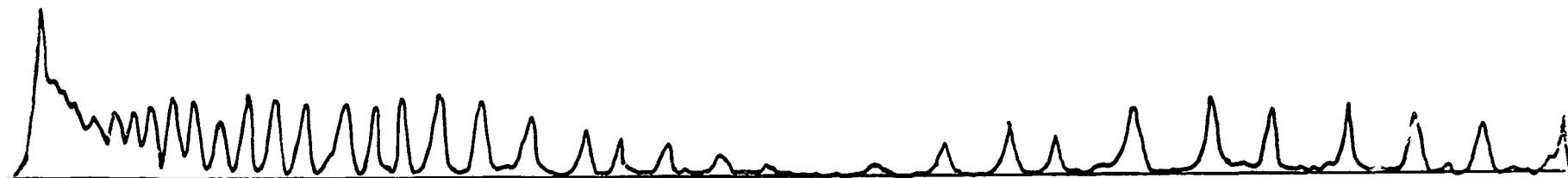


Figure 9. The laser induced fluorescence spectra of the X state of CN produced in the photolysis of cyanoacetylene.

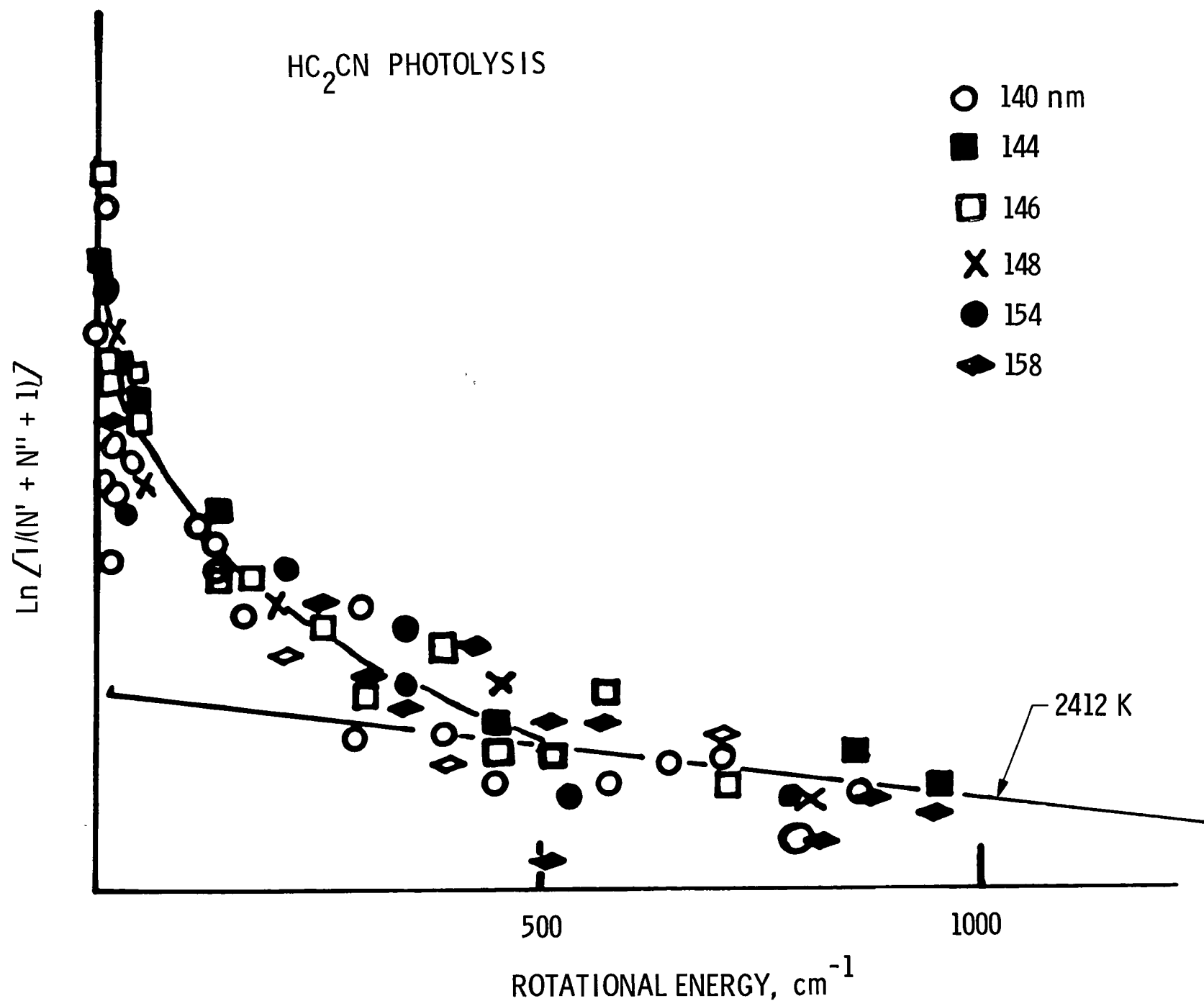


Figure 10. Boltzmann Plot of the rotational energy of the  $x$  state radical at the indicated wavelengths.

A simple picture emerges from this. First the energy that goes into excitation of the excited state does not have time to randomize or one would have to see increases in this rotational energy with increasing amounts of available energy. In  $C_2N_2$  and  $C_2HCN$ , 4,000 and 8,140  $cm^{-1}$  of additional energy is added to the excited state of the molecule yet the fraction that appears as energy in the CN rotation fragment barely changes. One might expect that randomization of energy would increase the amounts of energy going into the bending modes of molecules which in turn would, upon dissociation, increase the rotational energy. The results indicate that either coupling between the CN symmetric and the bending modes is weak or that randomization does not occur.

c.  $H_2O$

The results presented thus far suggest that as long as there is no change in the geometry of the molecule when the electronic transition occurs then the fragment will not be rotationally excited. It has been shown earlier by Carrington (9) that when  $H_2O$  is photolyzed at  $L_\alpha$  the  $OH(A^2\Sigma^+)$  fragment is produced rotationally excited. This rotational excitation is due to H-O-H bond angle opening up before dissociation. Welge and Stuhl (10) showed that in the first absorption region above 140 nm the ground state  $OH(X^2\Pi)$  was rotationally cool. In the latter work the study was done at pressures from 0.2 to 8.0 torr and the time delays were of the order of 0-5000 sec. Under these conditions it is possible that rotational relaxation had occurred before the radical was detected. The correlation diagram (11) in Figure 11, shows that both ( $B^1A_1$ ) state and the ( $^1B_1$ ) state correlate with  $OH(^2\Pi)$  through a linear symmetric intermediate  $^2\Pi_u$  state of  $OH$ . Since  $H_2O$  is so important in comets it is important to determine whether any rotationally excited  $OH(X^2\Pi)$  radicals are produced in the VUV photolysis of  $HOH$  between 140 to 170nm.

The experiment was performed by turning the VUV monochromator to the zeroth order so that broad band photolysis could be performed. Figure 12 shows that when the spectral output of our lamp is convoluted with the absorption spectra of  $HOH$  most of the absorption will occur in the region of the first continuum. Narrow band photolysis could be performed in the normal manner.

The results from the photolysis are shown in Figure 13 and they confirm the previous results reported by Welge and Stuhl. The rotational temperature determined from these observations is 1620K indicating the radical is produced rotationally cold. This is in agreement with results obtained from  $H_2S$ , a molecule with a similar electronic configuration and geometry as  $H_2O$ . In addition there is some evidence that the  $^2\Pi_{3/2}$  state is preferentially produced when compared to the  $^2\Pi_{1/2}$  state of  $OH$ . This also agrees with the  $H_2S$  results.

#### Summary

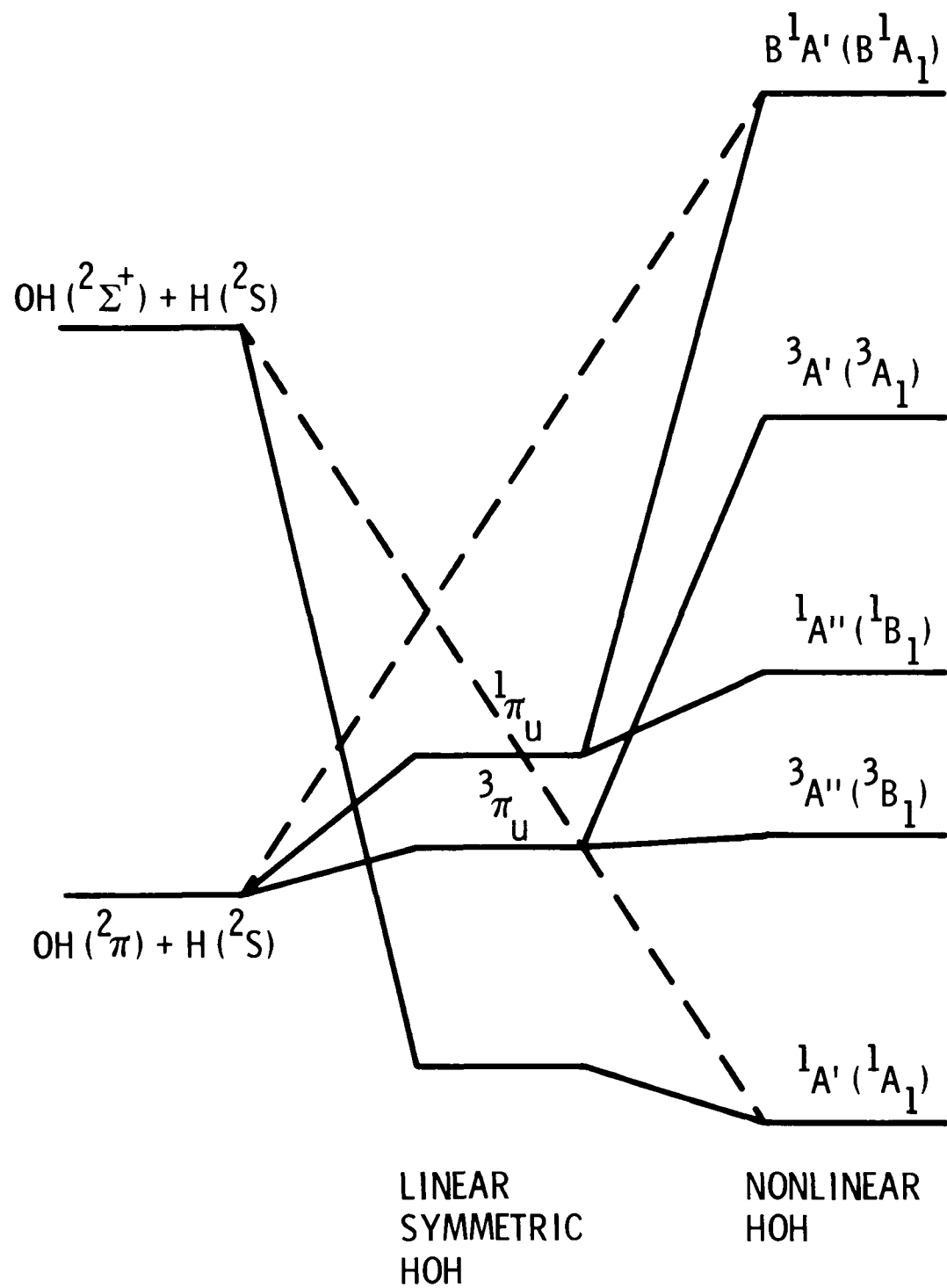
The results obtained thus far on the dynamics of photodissociation are in complete accord with the idea that extreme rotational excitation only occurs when the molecule executes large changes in geometry when it is electronically excited. This in turn suggests that true dynamical information can be used to determine this geometry.

This work has been supported in part in the planetary program under NASA Grant NGC-5071 and under ONR contract N00014-80-C-0305.

#### References

1. Jackson, W. and Cody, R. 1974, J. Chem. Phys. 61, 4183.
2. Jackson, W. 1974, "The Study of Comets" IAU Colloq. 25, 2, 679.
3. Connors, R. E., Roebber, J. L. and Weiss, Karl. 1974, J. Chem. Phys. 60, 5011.
4. Cody, R. J., Sabety-Dzvonik, M. J. and Jackson, W. M. 1977, J. Chem. Phys. 66, 2145.
5. Brunner, T. A., Smith, \_\_\_\_\_ and Pritchard, D. 1980, Chem. Phys. Lett. 71, 358.
6. Ashford, M. N. R. and Simons, J. P. 1977, J. Chem. Soc. Faraday Trans. 2, 73, 858.
7. Jackson, W. M. 1974, J. Chem. Phys. 61, 4177.

8. Cody, R. J. and Sabety-Dzvonik, M. J. 1976, 12th Informed Conference on Photochem., Washington, DC, E-4.
9. Carrington, T. 1964, J. Chem. Phys. 41, 2012.
10. Welge, K. H. and Stuhl, F. 1967, J. Chem. Phys. 46, 2440.
11. Howard, R. E., McLean, A. D. and Lester, W. A., Jr. 1979, J. Chem. Phys., 2412.



ADIABATIC CORRELATION DIAGRAM

AFTER HOWARD, MCLEAN AND LESTER      JCP 71 2412

Figure 11. Correlation diagram for water.

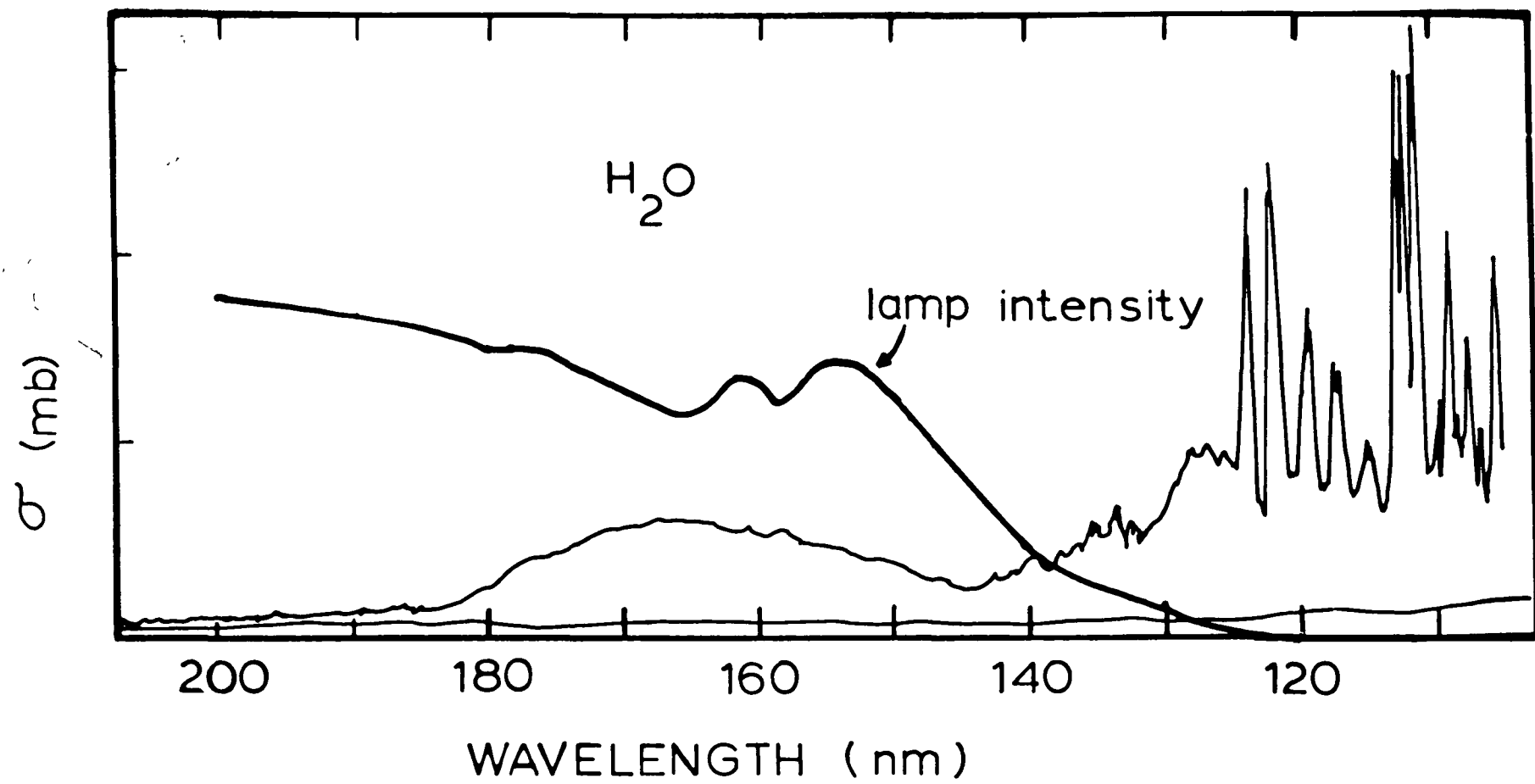
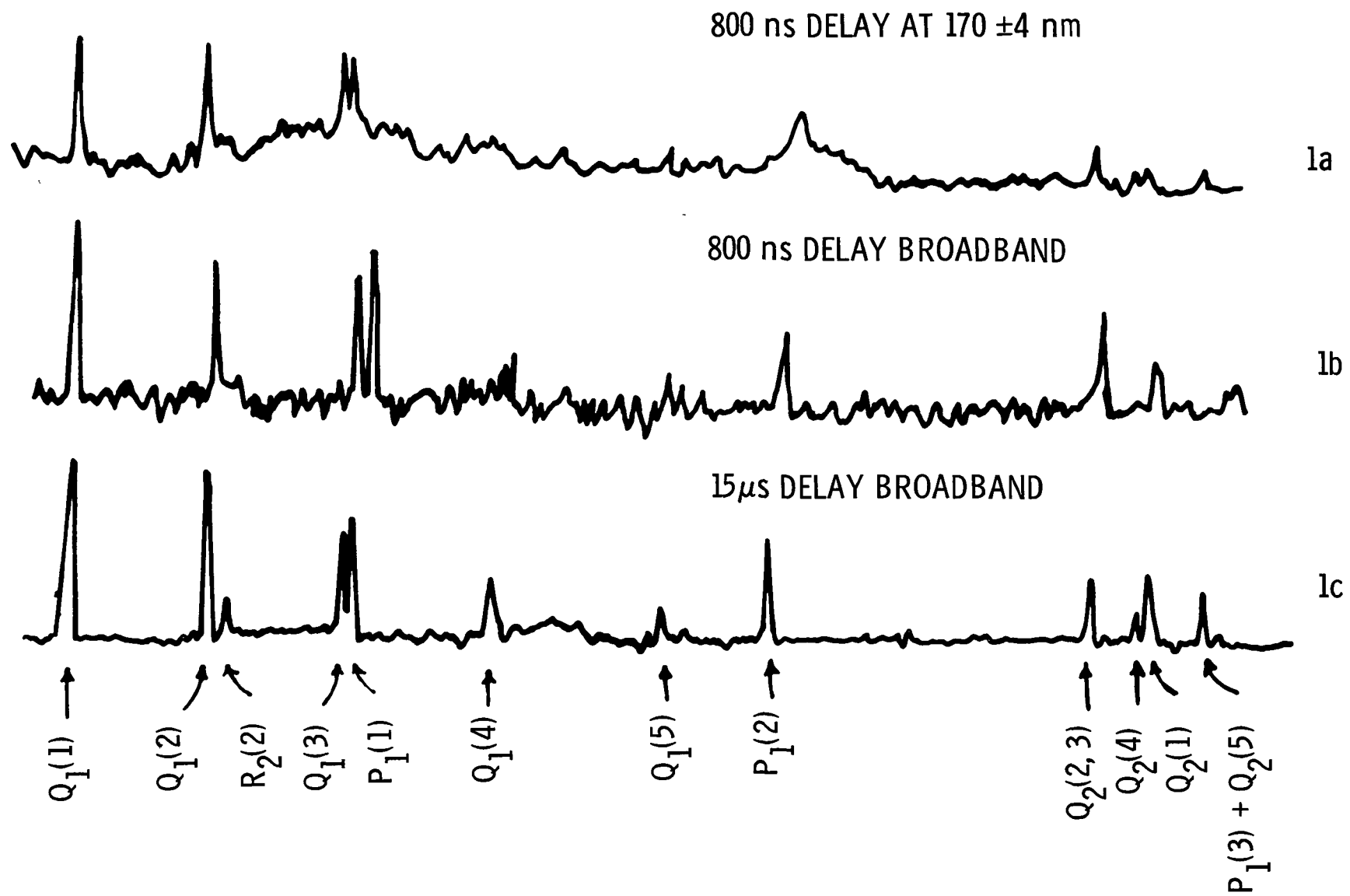


Figure 12. A convoluted wavelength profile of the absorption profile of water and the photolysis lamp profiles.



LIF SPECTRA OF OH  $A^2\Sigma \leftarrow X^2\Pi$  0-0 AT 306 nm  
 FOLLOWING PHOTOLYSIS OF WATER VAPOR

Figure 13. Laser induced spectra of the OH radical produced in the photolysis of water.